Numerical Modelling of Seismic Behavior of Retrofitted RC Beam-Column Joints

Seyyed Aliasghar Arjmandi [a*], Maryam Yousefi [b]

[a] Assistant Professor, University of Zanjan, Engineering Department, Zanjan, 45371-38791, Iran.

[b] M.Sc. Student, University of Zanjan, Engineering Department, Zanjan, 45371-38791, Iran.

Abstract

In the event of an earthquake, the beam-column joints in the reinforced concrete moment-resisting frame structures are affected by a high level of deformations and stresses. Due to these deformations and stresses, the joint can be damaged and even fractured in some cases. The failure of the beam-column joint can cause the building to collapse. In recent years, particular attention has been paid to strengthening joints in the substandard RC buildings. In this paper, the beam-column joint is investigated considering the nonlinear behavior for concrete and steel. For concrete, the damage plasticity model and for reinforcing steels bilinear plasticity model is used. Several examples of tested joints in the technical literature have been modeled before and after strengthening, then numerical and experimental results are compared. Seismic performance of joints has also been studied. The results of this research show good agreement between the results of finite element model and experimental results. Moreover, the retrofitting method have shown could improves the seismic performance of the joint.

Keywords: RC Beam-Column Joints; RC Joint Strengthening; Concrete Damage Plasticity; Nonlinear Material.

1. Introduction

The beam column joints due to experiencing cyclic deformations during an earthquake are one of the most critical parts of the RC moment-resisting frames. Hanson carried out the first experiments on beam-column joints in the 1960s [1]. Other researchers pursued Hanson works to improve the seismic performance of the RC joints. The results of researches carried out until 1976 led to the release of ACI-ASCE352. Today, also many studies are carrying out on the behavior of RC joints under earthquake loads or strengthening the joints in the existing non-conforming structures [2-7]. Pimanmas et al. studied the effect of joint area enlargement on the shear strength of the joint [8]. In their proposed method, joint area enlarged with monotonically cast square concrete. They concluded that the joint enlargement could increase the strength, stiffness and energy dissipation. Their experimental results indicated the decrease in joint shear stress in strengthened specimens. They also proposed a strut and tie model for analyzing joint area. Li et al. proposed rehabilitation of interior beam-column joints using ferrocement jackets with embedded diagonal reinforcements [9]. Their results have indicated that the proposed rehabilitation method can improve the seismic performance of interior beam-column joints. Agarwal et al. studied the effect of confinement due to transverse reinforcement and FRP jacketing on external beam-column joints, before and after retrofitting [10]. They concluded GFRP jacketing could be an effective technique to regain the strength and stiffness of damaged joints. Another research which is conducted by Del Vecchio et al. also used FRP for retrofitting of external joints [11]. Del Vecchio also proposed an analytical model to account for the strength increase provided by FRP systems in the seismic retrofit of poorly detailed corner joints [12]. Hejabi et al.

---

proposed a nonlinear procedure for analysis of FRP strengthened beam-column joint based on a softened truss model [13]. Karayannis has investigated the continuous rectangular spiral reinforcement applied as shear reinforcement in beam-column joints instead of the commonly used stirrups [14]. He obtained that rectangular spiral reinforcement has a better response in terms of the developing failure mechanisms, maximum loads and hysteretic energy absorption compared to the stirrups. Arzeytoon et al. presented a new seismic retrofitting method for beam-column joints based on the planner enlargement of the joint by using a steel plate, angles, and post-tensioning rods [15]. They show that the proposed retrofitting technique is effective and easy to install. Kalogeropoulos et al. experimentally and analytically investigate the effectiveness of a rehabilitation scheme for substandard exterior beam-column joints [16].

The retrofitting technique proposed in that research combines the improvement of the beam longitudinal reinforcing bars' anchorage in the joint, by using extension bars and steel plates and the reinforced concrete jacketing of the columns and the joint area. Their experimental results shows a substantial improvement of the overall seismic behavior of the joints retrofitted according to the proposed technique. Yurdakul and his coworker investigated the efficiency of the strengthening method using diagonal post-tension rods in external beam-column joints, which do not comply with any code requirements [17]. They used post-tension rods, which were mounted diagonally on each side of the joint and found that the lateral force capacities of the beam-column assemblies could be improved up to code requirements by the proposed rehabilitation scheme. However, their proposed method was not so applicable for the joints with transverse beams. Mostofinejad et al. have conducted an experimental study to investigate the effects of grooving method in the seismic behavior of exterior beam-column substandard joints strengthened with CFRP sheets taking advantage of the special technique of externally bonded reinforcement on grooves [18]. Their study reveals that application of CFRP composites on grooves was able to produce a significant enhancement in the seismic capacity of the test specimens. Lee et al. investigated beam-column joint behavior reinforced with high strength steel and concrete [19]. They found that the deformation capacity of beam-column joints could be increased by reducing the joint shear demand or increasing the joint transverse reinforcement ratio. Their study proposes several modifications to the existing design provisions for beam-column joints using high-strength reinforcement and concrete. Another studies using high strength concrete also is conducted with Liu et al. [20] and Alaee et al. [21]. Several numerical studies using finite element method have performed on the behavior of beam-column joints [3, 22]. In this study, exterior beam-column joints utilizing damage plasticity model for concrete and nonlinear plastic model for reinforcing steel bars and geometric nonlinearity effects are modeled in Abaqus. Considered analyzed cases are previously tested in half-scale. Subsequently, numerical and experimental results are compared.

2. Nonlinear Material Models

Reinforced concrete is one of the most complex materials in finite element modeling due to complicated nonlinear behavior in tension and compression. The correct definition of materials in finite element method modeling, in elastic and plastic behaviors as well as in compression and tension domains can have a great impact on the responses and outputs.

In this study, damage plasticity model is used for concrete. The model is a continuum, plasticity-based, damage model, which assumes that the main two failure mechanisms are tensile cracking and compressive crushing of the concrete material. The model assumes that the uniaxial tensile and compressive response of concrete is characterized by damaged plasticity, as shown in Figure 1.
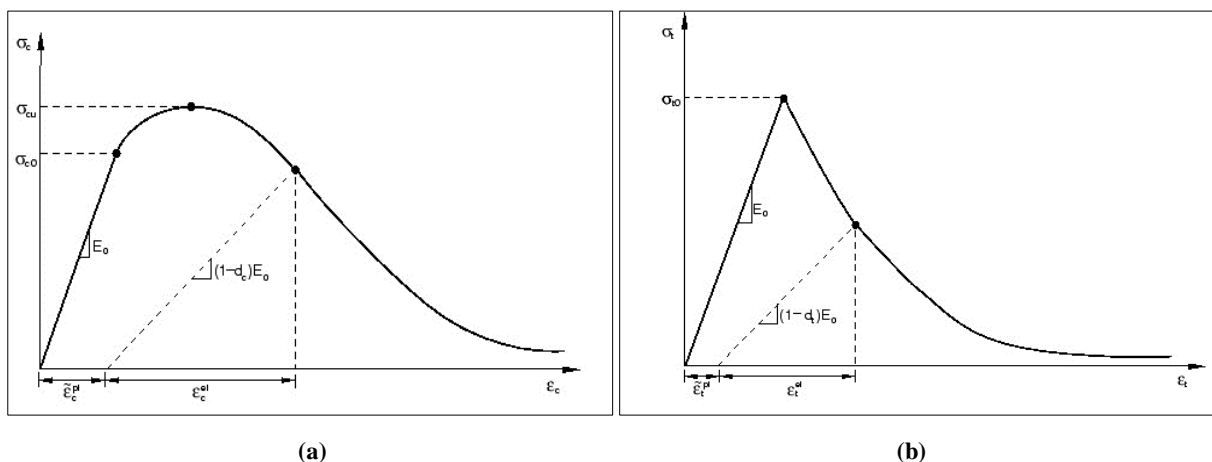

(a)   **(b)**

Figure 1. Response of concrete to uniaxial loading (a) in tension and (b) in compression

Under uniaxial tension, the stress-strain response follows a linear elastic relationship until the value of the failure stress σ_{t0} is reached. Beyond the failure stress, the formation of micro-cracks is represented macroscopically with a

softening stress-strain response, which induces strain localization in the concrete structure. Under uniaxial compression the response is linear until the value of initial yield σ_{c0}. In the plastic regime, the response is typically characterized by stress hardening followed by strain softening beyond the ultimate stress σ_{cu}. Some of the parameters required to define concrete behavior in tension is initial (undamaged) elastic stiffness of the material E_0 failure stress σ_{t0} and σ_t in terms of cracking strain ε_t^{ck} for softening branch. Cracking strain can be calculated from Equation (1):

$$\varepsilon_t^{ck} = \varepsilon_t - \varepsilon_{ot}^{el} \tag{1}$$

Where $\varepsilon_{ot}^{el} = \sigma_t / E_o$ is elastic strain corresponding to undamaged material and ε_t is total tensile strain. On the other hand, for compression behavior, it is required to define σ_c in terms of inelastic strain. Total strain can be converted to inelastic strain according to Equation (2):

$$\varepsilon_c^{in} = \varepsilon_c - \varepsilon_{ot}^{el} \tag{2}$$

In above equation $\varepsilon_{ot}^{el} = \sigma_c / E_o$ is the elastic strain corresponding to undamaged material and ε_c is total compressive strain.

As shown in Figure 1, when the concrete specimen is unloaded from any point on the strain-softening branch of the stress-strain curves, the unloading response is weakened: the elastic stiffness of the material appears to be damaged (or degraded). The degradation of the elastic stiffness is characterized by two damage variables, d_t and d_c, which are assumed to be functions of the plastic strains. These parameters have values between one, which shows the undamaged state of material and zero, which corresponds to completely damaged state. These parameters also should be defined in terms of plastic strains. For the reinforcing steel bars, bilinear plasticity model is used.

To define stress-strain curve for the concrete, the experimental stress-strain behaviors of tension and compression obtained by Velasco [23] are used. These curves are illustrated in Figure 2.
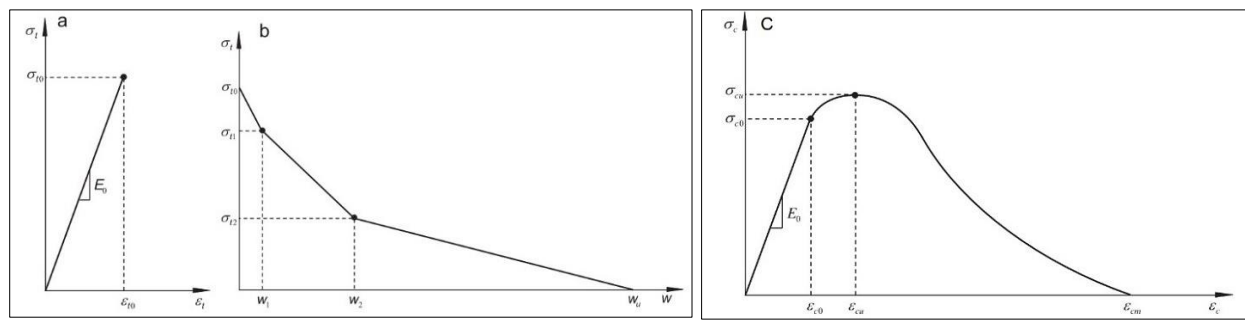

Figure 2. Ideal stress-strain curve for (a) uniaxial tension before crack initiation, (b) uniaxial tension post-failure and (c) uniaxial compression [23]

The tension behavior of concrete is defined by two curves, including one stress-strain curve before crack nucleation and another post failure stress-cracking displacement curve illustrated in Figure 2. The linear stress-strain relationship is expressed by $\sigma_t(\varepsilon_t) = E_0 \varepsilon_t$, $\varepsilon_t \leq \varepsilon_{t0}$ and the tri-linear model for stress-cracking displacement is determined by the following points, $(0, \sigma_{t0})$, (w_1, σ_{t1}), (w_2, σ_{t2}) and $(w_u, 0)$, where $\sigma_{t1} = k_1 \sigma_{to}$, $\sigma_{t2} = k_2 \sigma_{to}$, $w_1 = w_u / c_1$ and $w_2 = w_u / c_2$. k_1 and k_2 are the empirical parameters that can better describe the post-failure softening behavior in uniaxial tension test, while c_1 and c_2 are the constants, $c_1 = 20$ and $c_2 = 5$, respectively.

As proposed by Velasco, the ideal stress-strain curve under compression is composed by three sections: (a) initial elastic branch, (b) damage-based plastic rising branch and (c) damage-based plastic declining branch, illustrated in Figure 2, and the relations are given by the following equations:

$$\sigma_c(\varepsilon_c) = \begin{cases} E_o \varepsilon_c & \varepsilon_c \leq \varepsilon_o \\[2mm] \sigma_{cu}\left[1 - \left(1 - \dfrac{\varepsilon_c}{\varepsilon_{cu}}\right)^{\eta 1}\right] & \varepsilon_{co} \leq \varepsilon_c \leq \varepsilon_{cu} \\[2mm] \sigma_{cu}\left[1 - \left(\dfrac{\varepsilon_c - \varepsilon_{cu}}{\varepsilon_{cm} - \varepsilon_{cu}}\right)^{\eta 2}\right] & \varepsilon_{cu} \leq \varepsilon_c \leq \varepsilon_{cm} \end{cases} \tag{3}$$

Where ε_{cu} is the strain corresponding to the ultimate stress, $\varepsilon_{cm} = k_c \varepsilon_{cu}$ is the maximum strain in the ideal model, k_c is the empirical parameter obtained from the compression tests, $\eta 1$ and $\eta 2$ are the exponentials describing the curvatures

of rising and declining branches, respectively. Some other parameters required for concrete damage plasticity model are listed in Table 1.

In this research, reinforced concrete beam-column joints is modeled using Abaqus. Abaqus uses plastic damage model for concrete and required parameters are defined using Velasco model defined above.

Table 1. Some parameters for concrete damage plasticity model

Dilation Angle	Eccentricity	f_{b0}/f_{c0}	k_c	Viscosity
30°	0.1	1.16	0.667	0.001

3. Analyzed Models

The RC beam-column joints investigated in this research are joints of an analyzed five-story building. Half-scale specimens of these joints are experimentally investigated by shafaei et al. **Error! Reference source not found.**. In these research dimensions are selected similar to work of shafaei at al. **Error! Reference source not found.** for comparison purpose. The column section is 250×250 mm and has 2110 mm length. In addition, the beam section is a 250 × 220 mm rectangle and has 1400 mm length. Upper and lower longitudinal reinforcement bars of the beam are 4Φ14 and 3Φ14, respectively. Moreover, shear reinforcement for the beam is equally spaced Φ8 closed stirrups, starting at 25 mm distance from the column surface and spaced 60 mm from each other. The longitudinal reinforcement bars for the column are 8Φ14, and shear reinforcement for the column are equally spaced Φ8 closed stirrups with 60 mm distance from each other. Three types of exterior beam-column joints are considered: without shear reinforcement in the joint area, with shear reinforcement in the joint area and strengthened with post-tensioned steel angles. Material properties for the concrete and steel bars are as for Table 2 and Table **3**. Post-tensioning plate and angles have 18 mm thickness and post-tensioning bars have 16 mm diameter. Dimensions and reinforcement details for analyzed cases can be find in **Figure 3**.

Table 2. Material properties of modeled examples

Case Examples	Description	Compressive strength (MPa)	Tensile Strength (MPa)	Elastic Modulus (MPa)
C1	WO Shear reinforcement	23.3	3	22687
C2	W Shear Reinforcement	23	3	22540
C3	Strengthened With Steel Angles	25.3	3.1	23500

Table 3. Mechanical properties of reinforcement bars

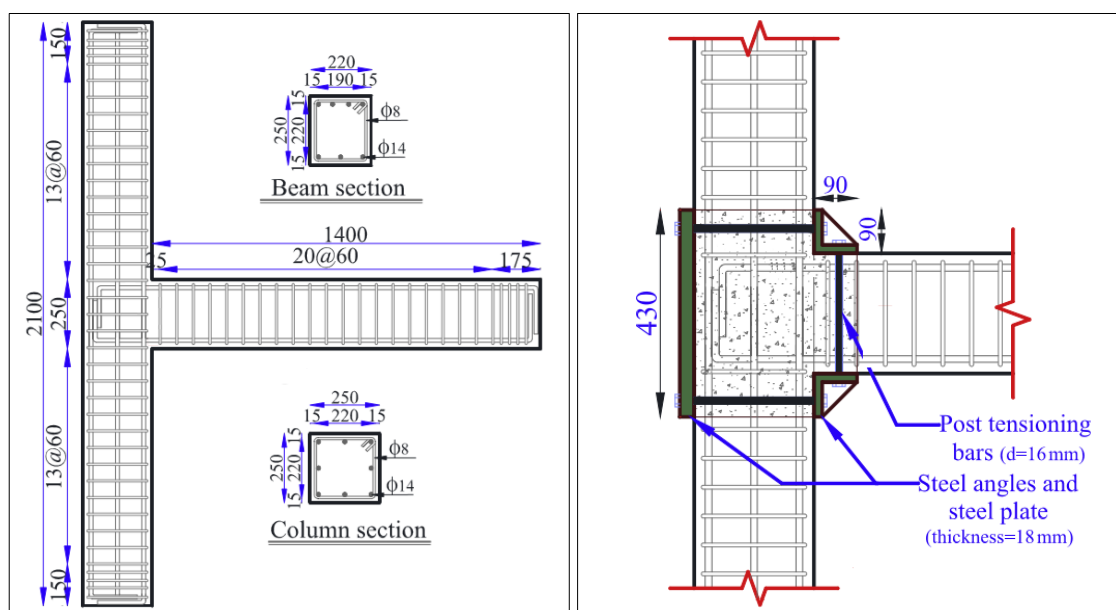| Bar diameter (mm)	Yield Strength (MPa)	Ultimate Strength (MPa)	Yield Strain (%)	Ultimate Strain (%)
8	350	410	0.18	18
14	460	680	0.2	13

Figure 3. Dimension and reinforcement details of analyzed models

4. Finite Element Modeling and Loading

Above mentioned three joints are models in plane stress condition. Plane stress condition is selected for simplicity and high computational time consumption of 3D models. Moreover, finite element discretization of analyzed cases are shown in **Figure 5**. For discretization of concrete domain and reinforcement bars, plane stress and link elements are used respectively. For discretizing concrete domain C3D4R quadratic four node elements and for steel bars T3D2 linear two node elements are utilized. The whole model is divided to three domains, two far of joint domains, upper and lower domains of the column, and near joint domain. The two far of joint domains have assigned linear material properties and near joint domain has nonlinear material properties. These can reduce computational time and convergence problems. The roller support condition is assumed for the end of the beam and for upper and lower ends of the column pinned condition are assumed. The nonlinear static analysis is conducted with displacement based cyclic loading. The incremental cyclic loading, which is shown in **Figure 4Error! Reference source not found.**, is applied at the end of the beam. Also axial load of the column is applied in the upper end of the column. It is noteworthy to mention that post-tensioning effect, which is required in C3, can be applied directly in Abaqus.
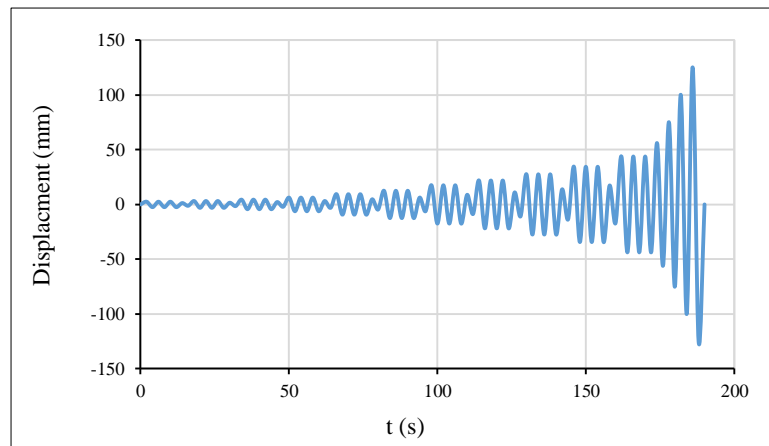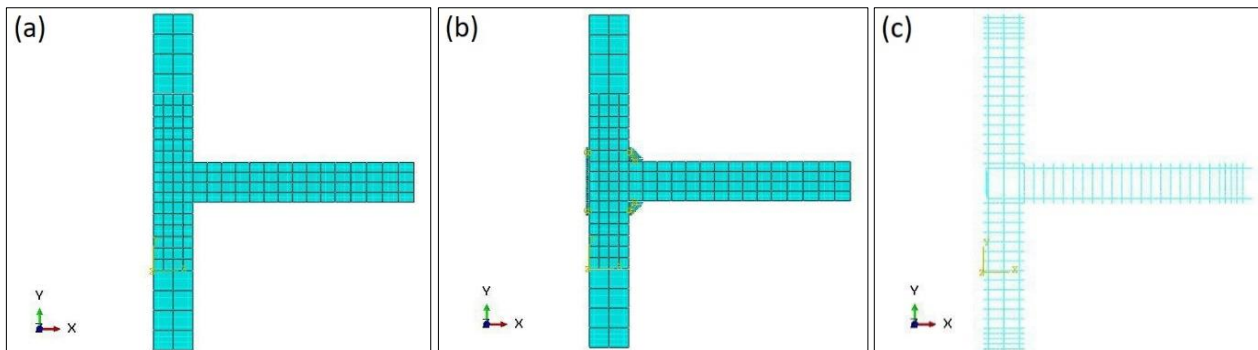

Figure 4. Incremental cyclic loading

Figure 5. Finite element discretization of analyzed models, (a) C1 and C2, (b) C3 and (c) reinforcement bars for C1

5. Results and Discussion

In **Figure 6** to**Figure 8**, the hysteresis response of the investigated joints both from experimental studies **Error! Reference source not found.** and numerical modeling are illustrated. In all cases, a good agreement between the experimental and the numerical results can be observed. In the elastic range, experimental and numerical results are almost coincident. However, in inelastic range, the curve of numerical results are located above the curve of the experimental results. Moreover, the pinching effect can be seen in hysteresis curves of the experimental results. This effect requires more details to be modeled and simulate in ordinary FEM modelings.
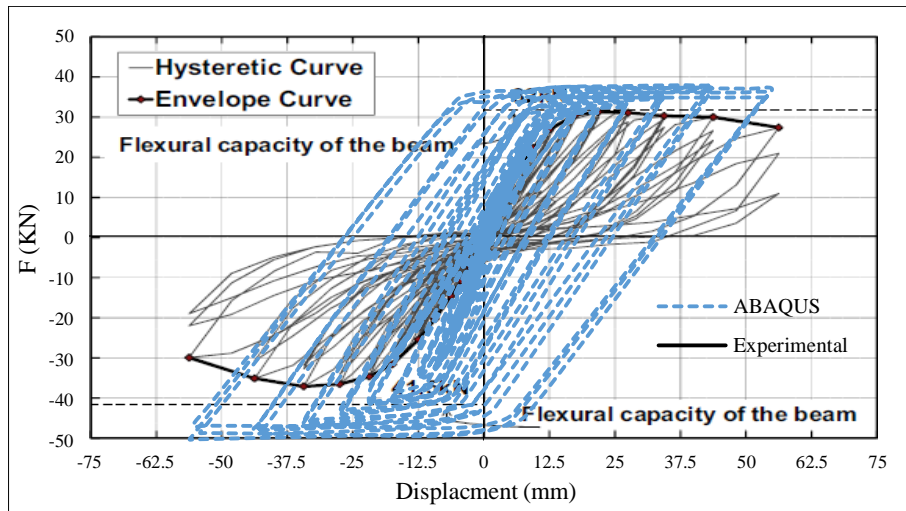
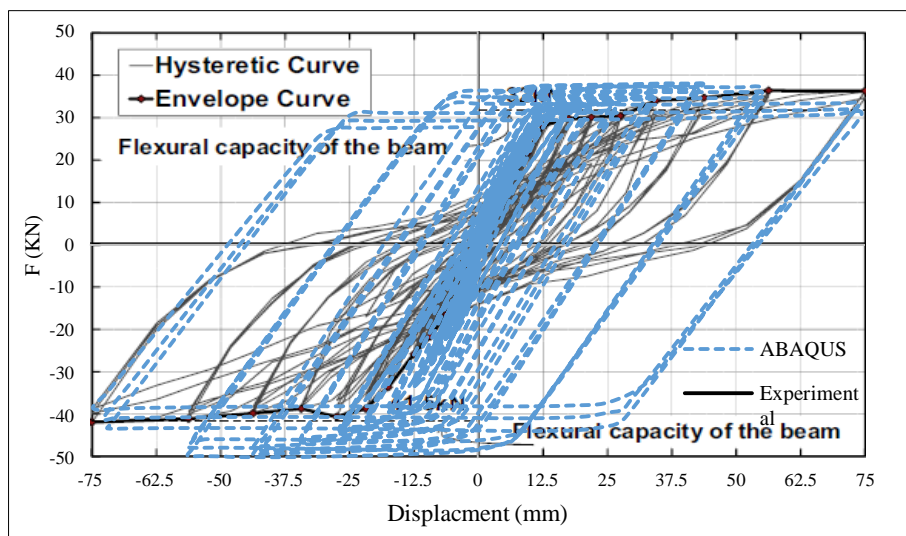**Figure 6. Hysteresis response of C1, numerical and experimental** Error! Reference source not found. **results**

Figure 7. Hysteresis response of C2, numerical and experimental Error! Reference source not found. **results**
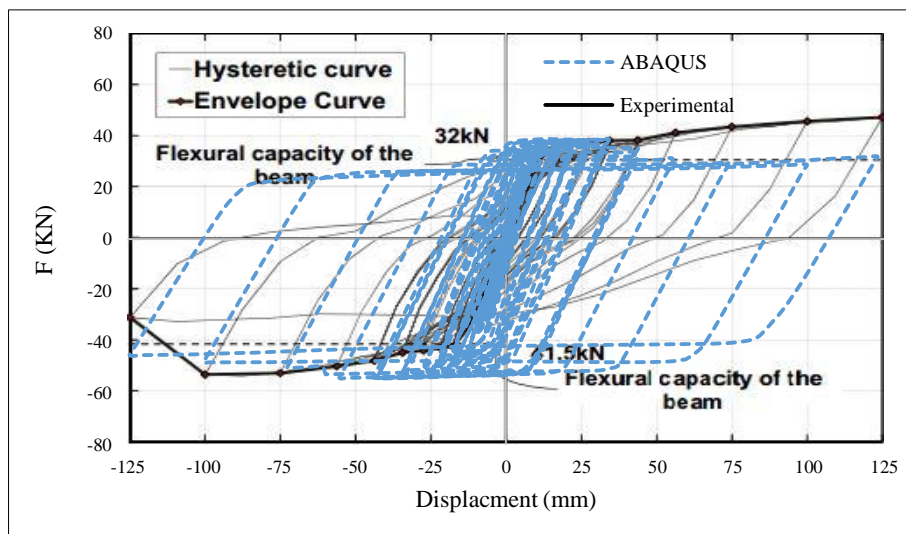

Figure 8. Hysteresis response of C3, numerical and experimental Error! Reference source not found. **results**

Hysteresis response or force-displacement curve during cyclic loading is the most important feature for evaluating the seismic performance of a structural component. It also can show energy absorption and ductility of the joint. The hysteresis response of C1 shows a decrease in stiffness and strength of the joint with increasing displacement, which results in shear failure of the joint. The C2 shows a ductile response and also had a slight stiffness degradation. The

hysteresis loops of the case reinforced with post-tensioned angles (C3) are clearly larger and remain stable with low stiffness and strength degradation. Differences between experimental and numerical results can be attributed to deficiency of utilized constitutive model for concrete and steel, some expected and accepted loss of accuracy for 2D modeling, not accounting for bond failure between concrete and steel, and other simplifications related to finite element discretization.

In **Figure 9** to**Figure 14**, damage parameter distribution in tension, d_t and in compression d_c at the end of analysis time are shown. In these figures failure can be recognized from element deformations and damage parameter intensity. As can be seen, for case C1, the shear failure occurred in the joint area and in the case of C2 and C3, shear failure is transferred to the column surface and the edge of strengthening angles, respectively.
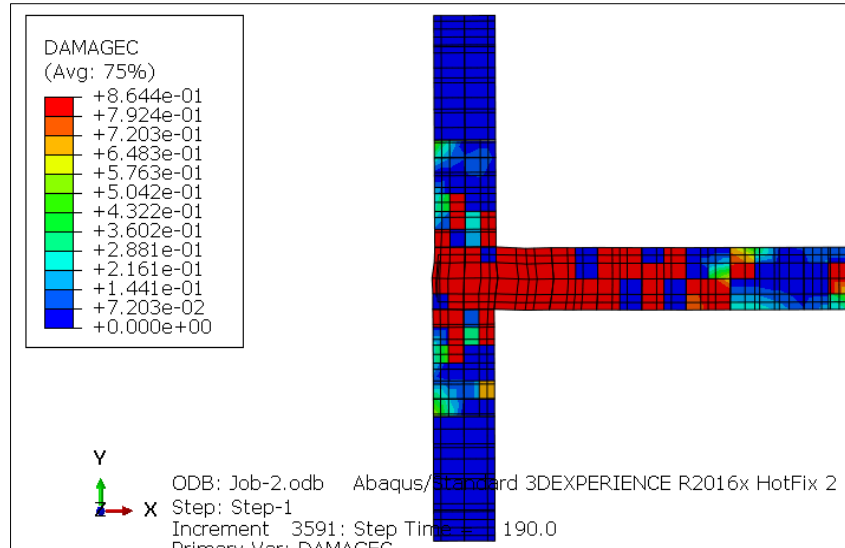

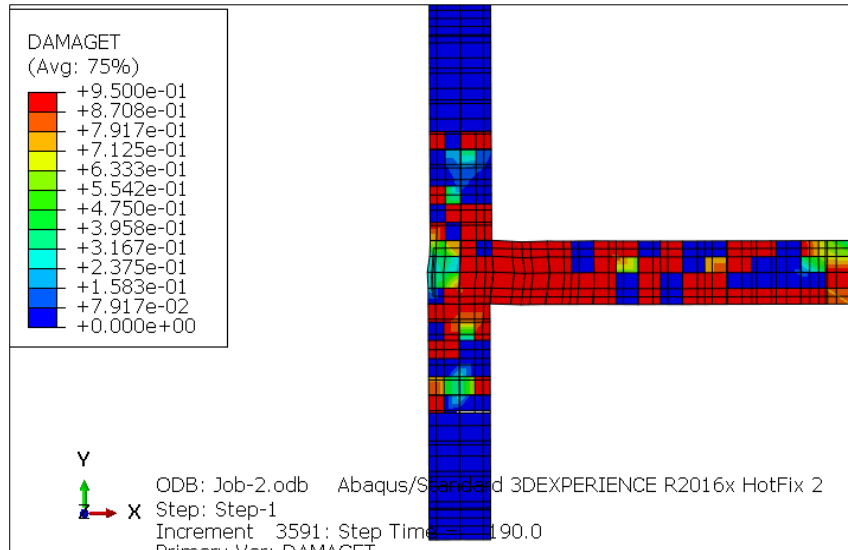**Figure 9. Compressive damage parameter for C1**

Figure 10. Tensile damage parameter for C1

Case C1 models an exterior joint without shear reinforcements. In some substandard buildings, unfortunately, the shear reinforcement is not implemented at the joint area. It can be understood from the deformations of the elements in the joint area (**Figure 9** and**Figure 10**) that these elements have been damaged in tension or compression. In other words, in this case, in contrast to the other two models that will be presented below, failure is in the joint's area, which can greatly decrease load capacity of the column.
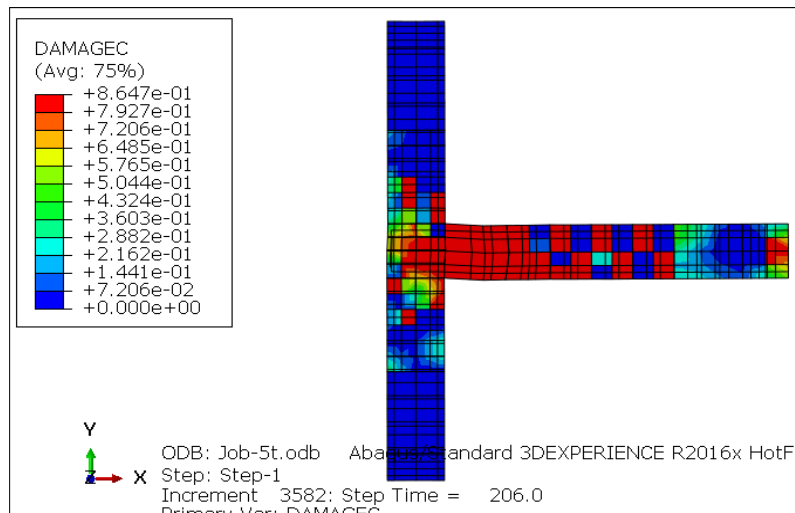
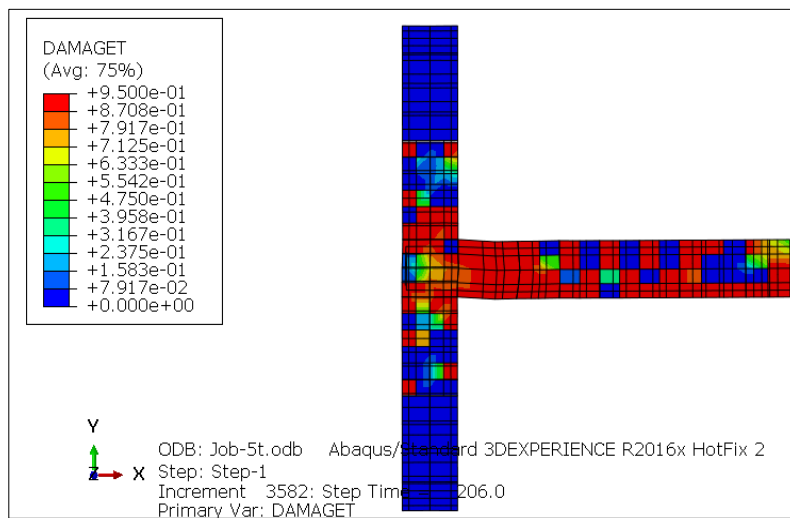**Figure 11. Compressive damage parameter for C2**

Figure 12. Tensile damage parameters for C2

The case C2 has modeled an exterior joint with shear reinforcement. Dimensions, other reinforcement and loading are similar to C1. According to **Figure 11** and **Figure 12** in this case, despite C1, the plastic hinge clearly moved into the beam. Although, according to the hysteresis diagram, the load-carrying capacity of the joint has not changed much, but its hysteresis loops are larger and, as a result, it is more ductile than C1.
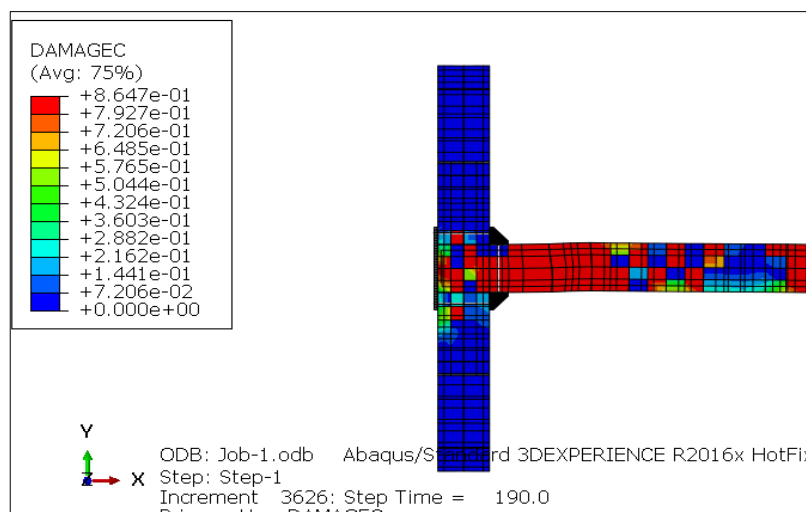

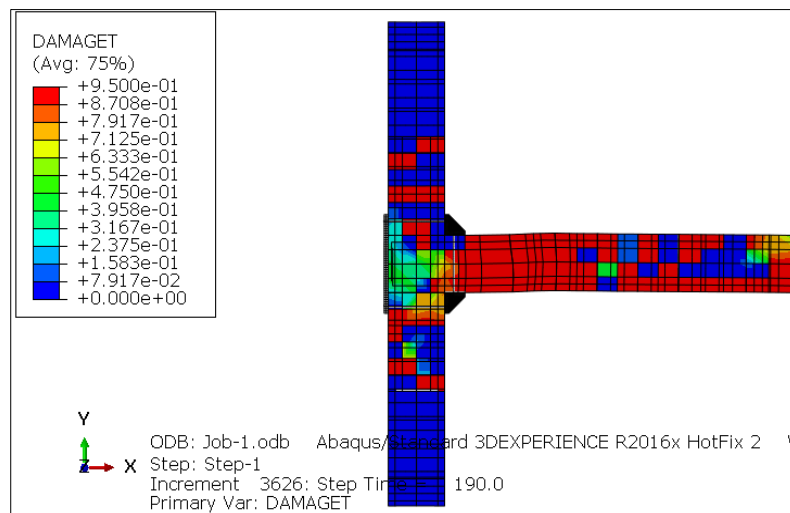**Figure 13. Compressive damage parameter for C3**

Figure 14. Tensile damage parameter for C3

Compressive and tensile damage parameters for case C3 are shown in **Figure 13** and **Figure 14**, respectively. Also hysteresis response of this model can be seen in **Figure 8**. C3 is model of an exterior joint retrofitted with steel plate, angles and post-tensioned bars. Element deformation shows that plastic hinge obviously moved out from the joint area. In addition damage parameters in the joint area are meaningfully lower than two previous cases. Despite C1, shear failure in the joint area do not occurred. This model has also been able to withstand larger deformations. This can be concluded from hysteresis response of **Figure 8**. Above results shows that post-tensioned angles is an effective and efficient solution for retrofitting RC beam-column joints without shear reinforcement.

6. Conclusion

In this research, seismic behavior of RC beam-column exterior joints are numerically investigated. Nonlinear behavior for concrete is considered in both tension and compression. Damage plasticity model is utilized for concrete material. Moreover, for reinforcement steel bilinear plasticity model is assumed. Three case examples for beam-column joint are modeled and analyzed: the joint without shear reinforcement in the joint area, with shear reinforcement and the joint with strengthening post-tensioned steel angles. Numerical results shows good agreement with the experimental results. It can be concluded that the shear reinforcement in the joint area can effectively increase ultimate strength and ductility of the joint. Results show that for joints without shear reinforcement, post-tensioned steel angles is a very effective and efficient solution. The retrofitted joint with post-tensioned steel angles shows a good behavior is cyclic loading. This can be attributed to concrete confinement and moving shear failure point to out of the joint area.

7. References

[1] Hanson, Norman W., and Harold W. Conner. "Seismic resistance of reinforced concrete beam-column joints." Journal of the Structural Division 93, no. 5 (1967): 533-560.

[2] Esmaeeli, Esmaeel, Fakhreddin Danesh, Kong Fah Tee, and Sassan Eshghi. "A Combination of GFRP Sheets and Steel Cage for Seismic Strengthening of Shear-Deficient Corner RC Beam-Column Joints." Composite Structures 159 (January 2017): 206–219. doi:10.1016/j.compstruct.2016.09.064.

[3] De Risi, Maria Teresa, and Gerardo Mario Verderame. "Experimental Assessment and Numerical Modelling of Exterior Non-Conforming Beam-Column Joints with Plain Bars." Engineering Structures 150 (November 2017): 115–134. doi:10.1016/j.engstruct.2017.07.039.

[4] De Risi, Maria Teresa, Paolo Ricci, and Gerardo M. Verderame. "Modelling Exterior Unreinforced Beam-Column Joints in Seismic Analysis of Non-Ductile RC Frames." Earthquake Engineering & Structural Dynamics 46, no. 6 (November 8, 2016): 899–923. doi:10.1002/eqe.2835.

[5] Chun, Sung-Chul, Chang-Sik Choi, and Hyung-Suk Jung. "Side-Face Blowout Failure of Large-Diameter High-Strength Headed Bars in Beam-Column Joints." ACI Structural Journal 114, no. 1 (January 2017). doi:10.14359/51689161.

[6] Behnam, Hamdolah, J.S. Kuang, and Roy Y.C. Huang. "Exterior RC Wide Beam-Column Connections: Effect of Beam Width Ratio on Seismic Behaviour." Engineering Structures 147 (September 2017): 27–44. doi:10.1016/j.engstruct.2017.05.044.

[7] Shayanfar, J., and H. Akbarzadeh Bengar. "Numerical Model to Simulate Shear Behaviour of RC Joints and Columns." Computers and Concrete 18, no. 6 (December 25, 2016): 877–901. doi:10.12989/cac.2016.18.6.877.

[8] Pimanmas, Amorn, and Preeda Chaimahawan. "Shear Strength of Beam–column Joint with Enlarged Joint Area." Engineering Structures 32, no. 9 (September 2010): 2529–2545. doi:10.1016/j.engstruct.2010.04.021.

[9] Li, Bo, Eddie Siu-shu Lam, Bo Wu, and Ya-yong Wang. "Experimental Investigation on Reinforced Concrete Interior Beam–

column Joints Rehabilitated by Ferrocement Jackets." Engineering Structures 56 (November 2013): 897–909. doi:10.1016/j.engstruct.2013.05.038.

[10] Agarwal, Pankaj, Ankit Gupta, and Rachanna G. Angadi. "Effect of FRP Wrapping on Axial Behavior of Concrete and Cyclic Behavior of External RC Beam Column Joints." KSCE Journal of Civil Engineering 18, no. 2 (March 2014): 566–573. doi:10.1007/s12205-014-0259-y.

[11] Del Vecchio, Ciro, Marco Di Ludovico, Alberto Balsamo, Andrea Prota, Gaetano Manfredi, and Mauro Dolce. "Experimental Investigation of Exterior RC Beam-Column Joints Retrofitted with FRP Systems." Journal of Composites for Construction 18, no. 4 (August 2014): 04014002. doi:10.1061/(asce)cc.1943-5614.0000459.

[12] Del Vecchio, Ciro, Marco Di Ludovico, Andrea Prota, and Gaetano Manfredi. "Analytical Model and Design Approach for FRP Strengthening of Non-Conforming RC Corner Beam–column Joints." Engineering Structures 87 (March 2015): 8–20. doi:10.1016/j.engstruct.2015.01.013.

[13] Hejabi, H., and M. Z. Kabir. "Analytical model for predicting the shear strength of FRP-retrofitted exterior reinforced concrete beam-column joints." Scientia Iranica. Transaction A, Civil Engineering 22, no. 4 (2015): 1363-1372.

[14] Karayannis, Chris G. "Mechanics of External RC Beam-Column Joints with Rectangular Spiral Shear Reinforcement: Experimental Verification." Meccanica 50, no. 2 (June 4, 2014): 311–322. doi:10.1007/s11012-014-9953-6.

[15] Arzeytoon, Ali, Abdollah Hosseini, and Alireza Goudarzi. "Seismic Rehabilitation of Exterior RC Beam-Column Joints Using Steel Plates, Angles, and Posttensioning Rods." Journal of Performance of Constructed Facilities 30, no. 1 (February 2016): 04014200. doi:10.1061/(asce)cf.1943-5509.0000721.

[16] Kalogeropoulos, George I., Alexander-Dimitrios G. Tsonos, Dimitrios Konstandinidis, and Stylianos Tsetines. "Pre-Earthquake and Post-Earthquake Retrofitting of Poorly Detailed Exterior RC Beam-to-Column Joints." Engineering Structures 109 (February 2016): 1–15. doi:10.1016/j.engstruct.2015.11.009.

[17] Yurdakul, Özgür, and Özgür Avşar. "Strengthening of Substandard Reinforced Concrete Beam-Column Joints by External Post-Tension Rods." Engineering Structures 107 (January 2016): 9–22. doi:10.1016/j.engstruct.2015.11.004.

[18] Mostofinejad, Davood, and Alireza Akhlaghi. "Experimental Investigation of the Efficacy of EBROG Method in Seismic Rehabilitation of Deficient Reinforced Concrete Beam–Column Joints Using CFRP Sheets." Journal of Composites for Construction 21, no. 4 (August 2017): 04016116. doi:10.1061/(asce)cc.1943-5614.0000781.

[19] Lee, Hung-Jen (Harry), and Chia-Jung Chang. "High-Strength Reinforcement in Exterior Beam-Column Joints Under Cyclic Loading." ACI Structural Journal 114, no. 5 (September 2017). doi:10.14359/51700788.

[20] Liu, Wei, and Jinqing Jia. "Experimental Study on the Seismic Behavior of Steel-Reinforced Ultra-High-Strength Concrete Frame Joints with Cyclic Loads." Advances in Structural Engineering 21, no. 2 (July 6, 2017): 270–286. doi:10.1177/1369433217717116.

[21] Alaee, Pooya, and Bing Li. "High-Strength Concrete Exterior Beam-Column Joints with High-Yield Strength Steel Reinforcements." Engineering Structures 145 (August 2017): 305–321. doi:10.1016/j.engstruct.2017.05.024.

[22] Faleschini, Flora, Paolo Bragolusi, Mariano Angelo Zanini, Paolo Zampieri, and Carlo Pellegrino. "Experimental and Numerical Investigation on the Cyclic Behavior of RC Beam Column Joints with EAF Slag Concrete." Engineering Structures 152 (December 2017): 335–347. doi:10.1016/j.engstruct.2017.09.022.

[23] Velasco, R. V. "Self-Consolidating Concretes Reinforced with High Volumetrics Fractions of Steel Fibers: Rheological, Physics, Mechanics and Thermal Properties." PhD diss., Ph. D. Thesis. COPPE, Federal University of Rio de Janeiro, Rio de Janeiro, 2008.

[24] Shafaei, Jalil, Abdollah Hosseini, and Mohammd Sadegh Marefat. "Seismic Retrofit of External RC Beam–column Joints by Joint Enlargement Using Prestressed Steel Angles." Engineering Structures 81 (December 2014): 265–288. doi:10.1016/j.engstruct.2014.10.006.